



Fractality, chaos, and reactions in imperfectly mixed open hydrodynamical flows

À. Péntek^a, G. Károlyi^b, I. Scheuring^c, T. Tél^d, Z. Toroczkai^{e,*},
J. Kadtké^a, C. Grebogi^f

^aMarine Physical Laboratory, Scripps Institution of Oceanography,
University of California at San Diego, La Jolla, CA 92093-0238, USA

^bDepartment of Structural Mechanics, Technical University of Budapest, Műegyetem rkp. 3.,
H-1521 Budapest, Hungary

^cDepartment of Plant Taxonomy and Ecology, Research Group of Ecology and Theoretical Biology,
Eötvös University, Ludovika tér 2, H-1083 Budapest, Hungary

^dInstitute for Theoretical Physics, Eötvös University, Puskin u. 5-7, H-1088 Budapest, Hungary

^eDepartment of Physics, University of Maryland, College Park, MD 20742-4111, USA

^fInstitute for Plasma Research, University of Maryland, College Park, MD 20742, USA

Abstract

We investigate the dynamics of tracer particles in time-dependent open flows. If the advection is passive the tracer dynamics is shown to be typically transiently chaotic. This implies the appearance of stable fractal patterns, so-called unstable manifolds, traced out by ensembles of particles. Next, the advection of chemically or biologically active tracers is investigated. Since the tracers spend a long time in the vicinity of a fractal curve, the unstable manifold, this fractal structure serves as a catalyst for the active process. The permanent competition between the enhanced activity along the unstable manifold and the escape due to advection results in a steady state of constant production rate. This observation provides a possible solution for the so-called “paradox of plankton”, that several competing plankton species are able to coexist in spite of the competitive exclusion predicted by classical studies. We point out that the derivation of the reaction (or population dynamics) equations is analog to that of the macroscopic transport equations based on a microscopic kinetic theory whose support is a fractal subset of the full phase space. © 1999 Elsevier Science B.V. All rights reserved.

1. Introduction

The advection of particles in time-dependent hydrodynamical flows is known to be typically *chaotic* [1–33]. If the particle takes on the velocity of the flow very rapidly,

* Corresponding author.

E-mail address: toro@k2.umd.edu (Z. Toroczkai)

i.e., inertial effects are negligible, we call the advection *passive*, and the particle a *passive tracer*. Its equation of motion is then

$$\dot{r} = v(r, t), \tag{1}$$

where v is the known velocity field. In stationary flows when the right-hand side is independent of t , problem (1) is integrable and the particle trajectories coincide with the streamlines of the flow. In time-dependent cases, however, streamlines and particle trajectories are *different*, and the latter ones can be much more complicated.

Here we consider passive advection in *open* flows [18–31], where the time-dependent region of the flow is assumed to be restricted to a *finite* domain, called the *mixing region*. While the tracer trajectories are simple outside the mixing region, they are typically chaotic inside of it.

It is worth emphasizing that a complicated flow field (turbulence) inside the mixing region is *not* required for a complex tracer dynamics. Even simple forms of time dependence, e.g. a periodic repetition of the velocity field in the mixing region is sufficient. The flow model we use here is of this type: in a finite domain the flow is time periodic with a period T , and outside this domain it is stationary.

In the following Section we show that the chaotic advection by open flows is associated with the appearance of stable *fractal* patterns. Then in Section 3 we argue that if the advected tracers are *active* in a chemical or biological sense, i.e. they can either react with neighboring particles or are subjected to a growth dynamics, then the activity mainly takes place along the same fractal set. This implies a new, novel form of surface reaction, which includes the parameters of the chaotic advection. Finally, in the concluding Section 4 we point out some possible applications of these results.

2. Advection of passive tracers in open flows

We consider open flows, where the flow is simple and stationary everywhere but in the mixing region. In the inflow and outflow regions the particle’s motion is simple, as they just follow the streamlines. In the mixing region, however, the particle paths can be very complicated and typically chaotic. As this chaotic behavior is restricted to a finite region both in space and time, it is necessarily of transient type. This *transient chaos* [34] is the most ubiquitous form of chaos which appears in open flows.

An important characteristic of such transiently chaotic systems is that tracers entering the mixing region are typically *trapped* there for long times. In fact, there is a set of tracer trajectories *never* leaving the mixing region. Among these non-escaping trajectories periodic orbits can be found with a period which is an integer multiple of the flow’s period T . Such periodic orbits are best visualized on a *stroboscopic map*, which is a series of snapshots taken at integer multiples of the flow’s period T . On the stroboscopic map the periodic tracer orbits of period mT trace out a series of m different points.

Of course, such permanently trapped orbits are quite exceptional, and they are all unstable. This means that most typically the tracers having entered the mixing region leave it after some — typically long — time. The non-escaping orbits, however, form a fractal set (a fractal “cloud” of points on the stroboscopic map), called the *chaotic saddle*. It is called “saddle” because, similar to a saddle-point, the unstable trajectories forming it can be reached from a set of exceptional initial tracer positions that converge to the non-escaping trajectories as time goes by. All other trajectories, however, are escaping into the outflow region sooner or later.

The union of all exceptional trajectories converging to the non-escaping orbits is the *stable manifold* of the chaotic saddle. The tracers starting from the close vicinity of the stable manifold are advected towards the chaotic saddle, and they follow some of the non-escaping orbits for a while. Once repelled from a non-escaping orbit, they might be trapped again by the stable manifold of another non-escaping orbit, exhibiting a kind of random walk among them. Finally, they leave the chaotic saddle along its *unstable manifold*. On the stroboscopic map, both the stable and unstable manifolds are complicatedly winding fractal curves [19–31] with some fractal dimension D_0 .

The unstable manifold can be directly observed both in experiments [35] as well as in environmental flows [36–38]. A droplet of tracers initially overlapping with the stable manifold is advected towards the chaotic saddle where it gets trapped for a long time.

The particles starting further away from the stable manifold are washed out quickly by the background flow, and they do not exhibit the kind of random walk among the orbits of the chaotic saddle. The tracers starting close to the stable manifold, however, spend a long time in the mixing region, and finally leave it along the unstable manifold of the chaotic saddle. This means that it is the unstable manifold where the tracers accumulate after sufficiently long time, as illustrated schematically in Fig. 1. This observation implies that although the chaos is transient in the mixing region, the particles trace out a *permanent fractal pattern*. If the unstable manifold is visualized by placing a single droplet of dye into the flow, the unstable manifold will be faded out as times goes by.

Indeed, the number of particles present in the mixing region decays exponentially in time with the exponent κ , which is called the *escape rate* [34]:

$$N(t) = N(0)e^{-\kappa t} . \quad (2)$$

The reciprocal of κ can be considered to be the average lifetime of transient chaos [34], and $1/\kappa$ is the average time a tracer spends in the mixing region.

As an illustrative example, we consider the flow of a viscous fluid around a cylinder with a background velocity pointing along the x -axis. At intermediate background velocities (whose dimensionless measure, the Reynolds number is of the order of 10^2) no stationary velocity field is stable, instead, a strictly periodic behavior sets in with period T , see Fig. 2. Two vortices are created behind the cylinder within each period, one above and another one below the x -axis. These two vortices are delayed by a time

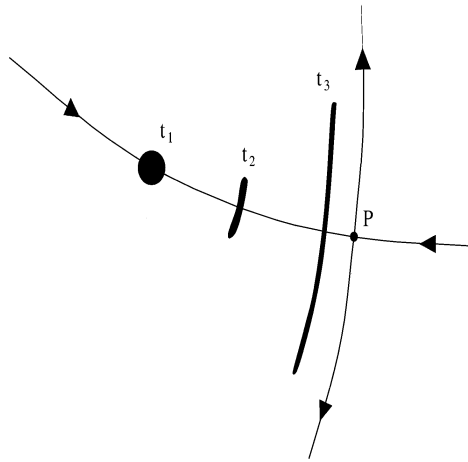


Fig. 1. Schematic illustration of a droplet of dye converging to the unstable manifold of the chaotic saddle. Point P illustrates a point of the saddle, while the two intersecting lines represent the stable and unstable manifolds. The droplet overlapping with the stable manifold at t_1 stretches as time goes on. The points on the stable manifold move towards P , while the other points are repelled from it along the unstable manifold.

$T/2$. The vortices first grow in size, then detach from the cylinder and start to drift downstream. This alternating separation of vortices from the upper and lower cylinder surface is called the *von Kármán vortex street* and is characterized by a strictly periodic velocity field of period T [39].

After a short length of travel, the vortices are destabilized and destroyed due to the viscosity of the fluid. Far away from the cylinder upstream and downstream the flow is practically stationary. The mixing region is thus located in the wake of the cylinder.

To obtain the velocity distribution one has to solve the two-dimensional viscous Navier–Stokes equations with no-slip boundary condition along a circle [20–22]. For simplicity we use here an analytic model for the streamfunction introduced in Ref. [22] motivated by a direct numerical simulation of the Navier–Stokes flow carried out by Jung and Ziemniak [21] at Reynolds number 250.

In Fig. 3 two particle trajectories are shown, with initial conditions deviating by an amount on the order of $10^{-3}R$. The trajectories diverge from each other rapidly, one leaves the wake at the top side, the other one at the bottom side of the cylinder. The typically exponential growth of the distance between initially close particles is a unique sign of the chaotic tracer motion, although the flow itself is strictly periodic, without chaoticity.

Fig. 4 shows a snapshot of the chaotic saddle and its stable and unstable manifolds in the wake of the cylinder. The chaotic saddle consist of a countable infinite number of periodic orbits and an uncountable number of non-periodic orbits. Tracers inserted on any black dot in Fig. 4a stay in the wake forever.

Particles inserted exactly on the stable manifold (Fig. 4b) converge to trajectories of the chaotic saddle after infinitely long time. If a tracer is, however, inserted off the

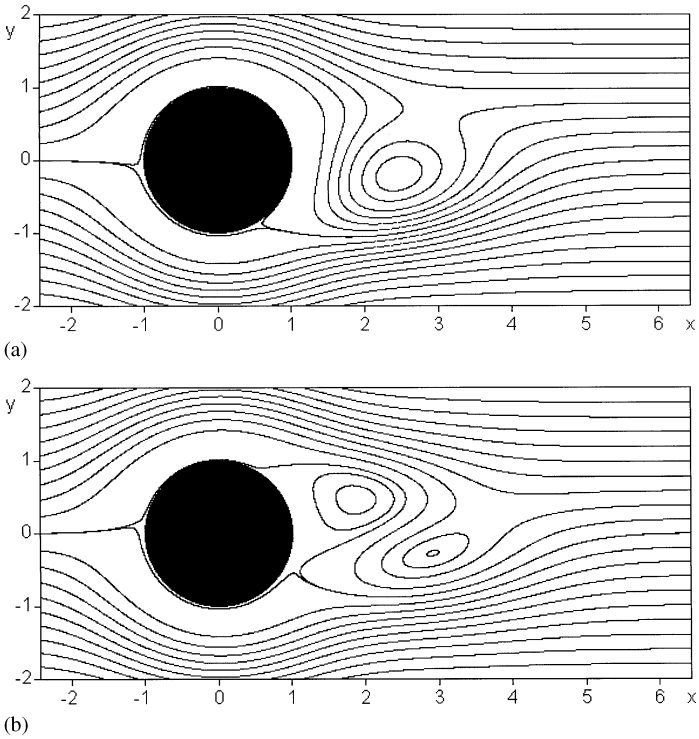


Fig. 2. Snapshots taken at times $t = 0 \pmod{T}$ and $t = T/4 \pmod{T}$ on the streamlines of the von Kármán vortex street. The fluid flows from left to right. During the first half time period ($T/2$) a vortex is born at the top side of the cylinder, while the vortex at the bottom side dies out due to viscosity. The streamlines at times $t = T/2 \pmod{T}$ and $t = 3T/4 \pmod{T}$ are the mirror images of these figures with respect to the $y = 0$ axis.

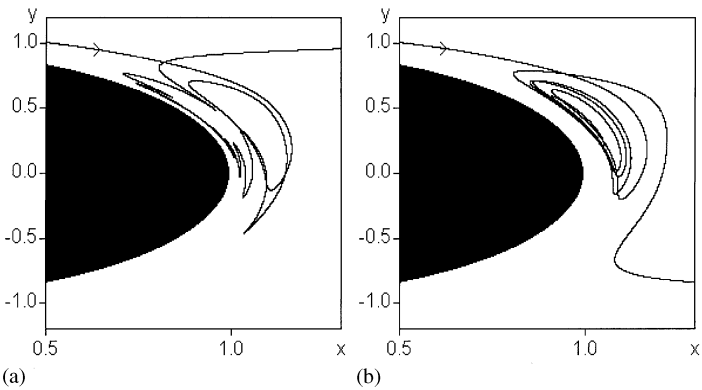


Fig. 3. Two particles initially close to each other trace out completely different paths. The cylinder is elongated in the horizontal direction for better visualization.

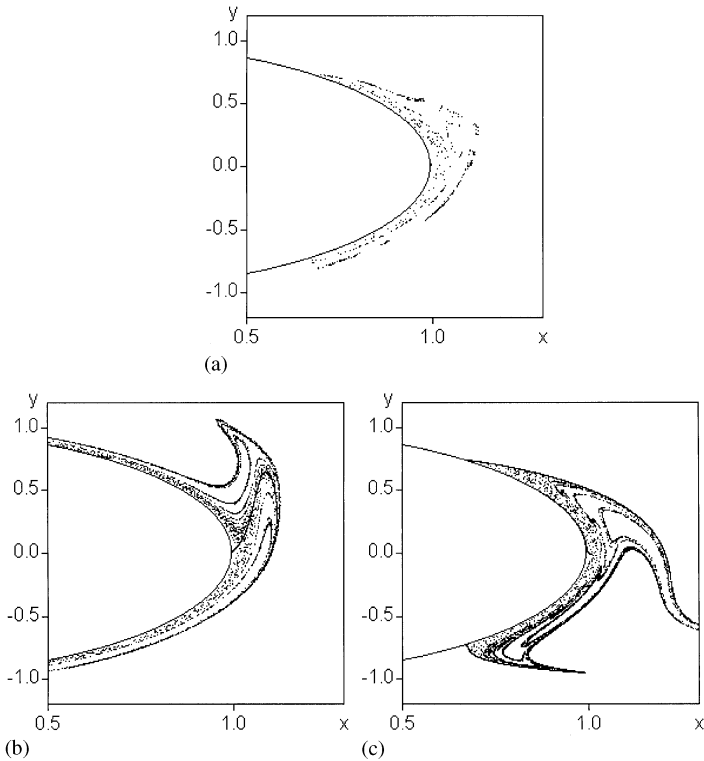


Fig. 4. The chaotic saddle (a) and its stable (b) and unstable (c) manifolds are shown on snapshots taken at $t = 0(\text{mod } T)$. While the chaotic saddle is a fractal cloud of points, its stable (unstable) manifold is a complicated curve reaching in the far upstream (downstream) region. The cylinder is elongated in the horizontal direction for better visualization.

stable manifold, but very close to it, it leaves the wake along the unstable manifold (Fig. 4c).

The unstable manifold is traced out by an ensemble of trajectories initially overlapping with the stable manifold. This is illustrated in Fig. 5, where the tracers still present in the mixing region are shown after some time. As tracers spending a long time in the wake of the cylinder, that is, being trapped in the mixing region, finally leave it along the unstable manifold, it is natural to expect that any kind of transport processes occurring mainly take place along this fractal set. This can indeed be seen in laboratory experiments [15]. The above-mentioned property of the tracer dynamics implies that classical flow visualization techniques based on dye evaporation or streaklines trace out fractal curves (unstable manifolds) which are *different from streamlines* or any other characteristics of the Eulerian velocity field (for several flow visualization photographs of this type see Ref. [39]).

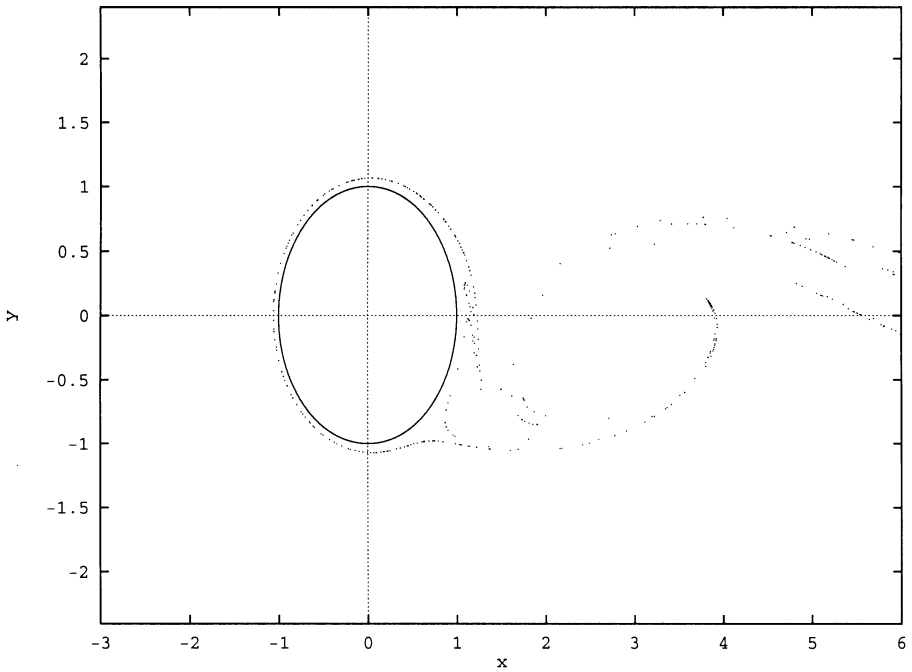


Fig. 5. The unstable manifold of the chaotic saddle is traced out by the tracers injected into the flow in front of the cylinder. The coverage is not perfect due to the finite number of particles. Initially 300×300 particles were inserted into the flow in the region $x \in [-2.55, -2.45]$, $y \in [-0.1, 0.1]$, and, for computational simplicity, their time-evolution was observed on a grid of size $1/300$. The snapshot was taken at $t = 2T$, where T is the period of the flow.

3. Advection of active tracers in open flows

In this section we consider the effect of the chaotic advection on the active processes on the flow's surface described by *kinetic reactions* [40,41]. Tracers injected into the flow are advected passively, they do not influence the flow. If, however, they come closer to each other than a given reaction distance σ , they interact with each other, creating thus the *product* particles. For our discussions we consider the *autocatalytic* reaction: $A + B \rightarrow 2B$. We insert a tiny seed of reacting B tracers into the flow covered with A particles. This way the reaction events occur on the surface between the areas covered by A and B particles: the A -type tracers become B within a distance σ . This distance can be considered as a *reaction range*. For computational simplicity the instantaneous reactions occur at integer multiples of a time lag τ , during which only advection occurs.

Fig. 6 shows the spreading of reagents B in the wake of the cylinder after a long time. The initial position of the tracers is the same as in Fig. 5. After a short transient (of about $4T$) a steady state is reached, which implies a constant production rate of B tracers in the wake. Note that the active tracers also trace out the unstable manifold,

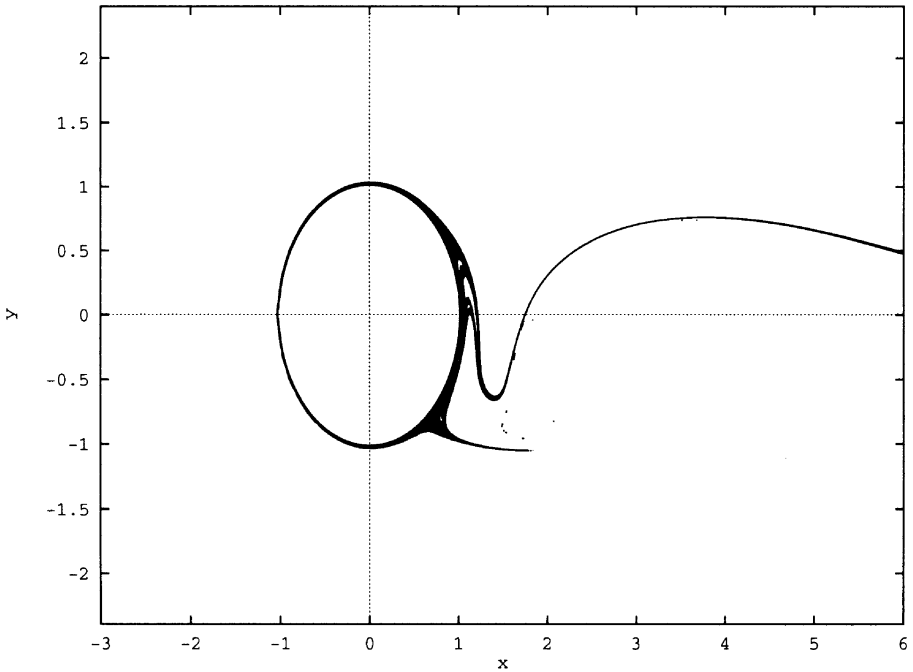


Fig. 6. The unstable manifold of the chaotic saddle is traced out by the autocatalytic tracers (B , black) injected into the flow in front of the cylinder. The coverage is much more efficient than in Fig. 5 due to the reactions. Initially 300×300 B particles were inserted into the flow in the region $x \in [-2.55, -2.45]$, $y \in [-0.1, 0.1]$, the rest of the fluid surface was covered by A . For computational simplicity, the time evolution was observed on a grid of size $1/300$. The snapshot was taken at $t = 20T$, where T is the period of the flow. The model parameters were $\sigma = 1/150$, $\tau = T/5$.

but the coverage is much wider due to the autocatalytic reactions. This means that the reactions occur *on the surface of a fattened-up fractal*.

Based on this observation, a simple theory [42,43] can give the area $\mathcal{A}_B(t)$ covered by the reacting tracers in the mixing region at time t . By taking the limit $\tau \rightarrow 0$, $\sigma \rightarrow 0$ but keeping σ/τ finite, a time continuous reaction equation can be obtained:

$$\dot{\mathcal{A}}_B = -\kappa \mathcal{A}_B + g \frac{\sigma}{\tau} \mathcal{A}_B^{-\beta}. \tag{3}$$

Here g is a constant, and

$$\beta = \frac{D_0 - 1}{2 - D_0} \tag{4}$$

is a nontrivial, positive exponent depending only on the fractal dimension D_0 of the unstable manifold. If the reactions occur along a simple line, that is, the surface between the A and B particles is not a fractal, we have $D_0 = 1$. This implies, via $\beta = 0$, that (3) describes a classical surface reaction [44] with reaction front velocity σ/τ in the presence of the escape (κ) of the products.

The negative exponent $-\beta$ in Eq. (3) implies that the reactions are enhanced due to the fractal boundary between the different reagents. In fact, the less reagent is present

in the mixing region, the more effective the reactions become because of the larger resolved surface. This leads to a balance between the escape due to advection (first term) and the production due to reactions (second term in (3)). Since in our case the long-time advection dynamics is concentrated on a fractal, the unstable manifold of the passive flow, we obtain essential deviations from traditional chemical or population dynamics theories derived for a well-stirred environment. These observations might be of relevance for other applications of statistical physics where the support of the underlying kinetic theory is not a smooth subset of the full phase space.

Via direct substitution, one can check that the solution to Eq. (3) is

$$\mathcal{A}_B(t) = \left(\frac{g\sigma}{\kappa\tau} - K e^{-\kappa/(2-D_0)t} \right)^{2-D_0}, \quad (5)$$

where K is an integration constant, and it is related to the initial area $\mathcal{A}_B(0)$ via

$$K = \frac{g\sigma}{\kappa\tau} - [\mathcal{A}_B(0)]^{1/(2-D_0)}. \quad (6)$$

One can see from solution (5) that in the long-time limit $t \rightarrow \infty$, the area will be expressed as $(\varepsilon^*)^{2-D_0}$, i.e., as a coverage of the fractal unstable manifold with stripes of a *non-zero* average width $\varepsilon^* = g\sigma/\kappa\tau$. In case of no chemical reactions ($\sigma = 0$), we obtain the usual exponential emptying dynamics with κ being the escape rate, just as expected. The appearance of a novel term in the chemical rate equation is a macroscopic consequence of an underlying kinetic theory. In contrast to the classical theory, however, the chemically active tracers occupy a fractal subset of the full phase space (the unstable manifold) only.

The balance mentioned above can serve as a possible answer for a long-standing question called the *paradox of plankton* [45]. In well-mixed environments, classical studies [46,47] predict that all competing species die out except the most perfectly adapted ones for all the limiting factors. As the number of different limiting factors is rather small (on the order of 10), it is quite surprising that the number of different competing plankton populations is quite large. The keyword in the above problem is “well-mixed environment”. We have seen that in open flows the advected tracers are *not* well-mixed, instead, they form a structured spatial distribution of tracers. It is thus natural to expect that in open flows, when the activity (in this biological sense the competition) is restricted to the surface of a fattened-up fractal, the number of competing species can be larger than the number of limiting factors.

The competition in our case is modeled by two autocatalytic reactions $A + B \rightarrow 2B$ and $A + C \rightarrow 2C$ using the same resource A , which is the only limiting factor. Both species have different replication abilities σ_B and σ_C , and mortality rates δ_B and δ_C . The mortality rate is the probability that an organism dies out during the time lag τ . In a well-mixed environment, the traditional theory implies that only species B or C survives the competition, the one with superior reproduction abilities. In open flows, as illustrated in Fig. 7, the coexistence of the competing species B and C can be observed. Both species are present in the wake of the cylinder, thus both of them are pulled along the unstable manifold. Here their activity is enhanced, which leads to increased access for both species to the background material A for which they compete.

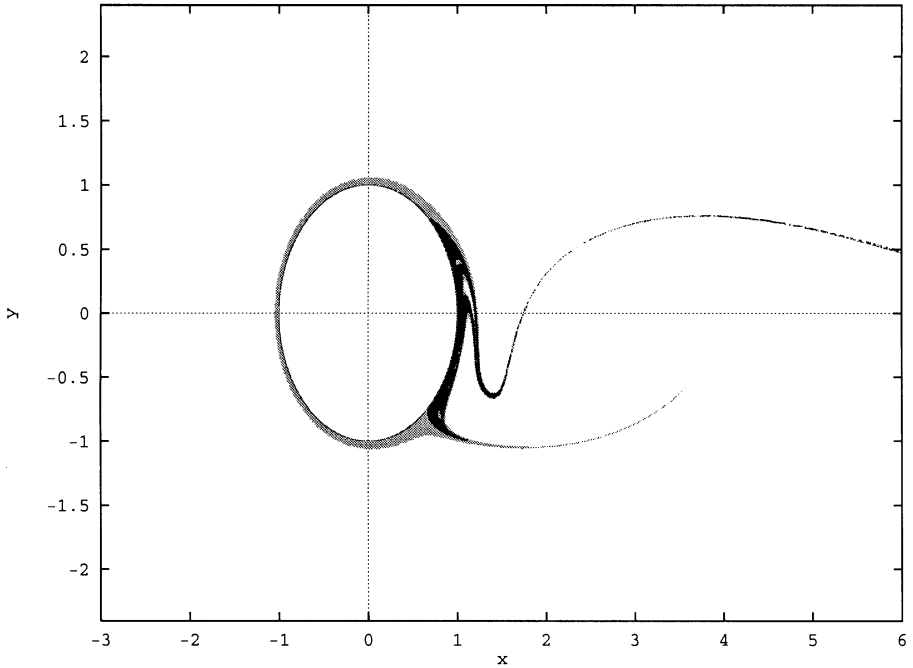


Fig. 7. The unstable manifold of the chaotic saddle is covered by the competing species *B* (light-grey) and *C* (dark-grey) at time $t=20T$, after reaching the steady state. The background material *A* is shown in white. Initially 300×300 *B* particles were inserted into the flow in the region $x \in [-2.55, -2.45]$, $y \in [0, 0.1]$, and 300×300 *C* particles in the region $x \in [-2.55, -2.45]$, $y \in [-0.1, 0]$. The grid size chosen was $1/300$. The model parameters were $\sigma_B = 1/150$, $\sigma_C = 1/300$, $\delta_B = 0.5$, $\delta_C = 0.0001$, and $\tau = 0.2T$.

Thus, due to the fact that the mixing of the different species is *not perfect*, coexistence along the unstable manifold is ensured [48] in a wide range of parameter *differences* characterizing the activity of the species.

4. Discussion

We have seen that particles advected by open flows trace out complicated fractal patterns. The particles spend a long time here, and they possess a largely increased surface to perform any kind of (chemical or biological) activity. Active tracers (chemical reagents or biological species) thus fatten-up the unstable manifold, and the major part of the activity takes place on a fractal set. Such processes have been observed e.g. in atmospheric chemistry, like the ozone depletion at the polar vortex. Here the filamental spatial distribution of ClONO_2 at the vortex edge [36,38] might be identified as the result of a reaction $\text{ClO} + \text{NO}_2 \rightarrow \text{ClONO}_2$ along a fractal. Similarly, in aquatic systems, the evolution of plankton populations was also reported to possess filamental spatial distribution [49–52].

Although the environmental flows are often thought of as *closed* ones (in the sense that there is no escape), they can still produce filamental spatial distribution, cf. [53,54]. One reason for this is that on the time-scale of the active environmental processes, and in a fixed frame of observation, these large-scale flows can be considered to be open with a net current flowing through the observation region. Additionally, there is no significant feedback into the region of observation on the time-scale of the active processes.

When the activity takes place along a non-trivial fractal boundary, a new kind of surface reaction equation (3) has been derived. It contains important chaos parameters, like the escape rate κ and the fractal dimension D_0 . These parameters, however, depend uniquely on the parameters of the hydrodynamics, like the Reynolds number. This equation, based on microscopic properties of the advection dynamics, gives a global, macroscopic description of the product depending only measurable quantities. This can lead to estimation of observable quantities that could provide a verification of the theory.

Acknowledgements

This research has been supported by the NSF-MRSEC at University of Maryland, by the NSF-DMR, by ONR(physics), CNPq/NSF-INT, by the DOE, by the US-Hungarian Science and Technology Joint Fund under Project numbers 286 and 501, by the Hungarian Science Foundation T019483, T025793, T029789, and F029637, by the Hungarian-British Intergovernmental Science and Technology Cooperation Program GB-66/95, and by the Hungarian Ministry of Culture and Education under grant number 0391/1997.

References

- [1] H. Aref, *J. Fluid Mech.* 143 (1984) 1.
- [2] H. Aref, S. Balachandar, *Phys. Fluids* 29 (1986) 3515.
- [3] J. Chaiken, R. Chevray, M. Tabor, Q.M. Tan, *Proc. Roy. Soc. London A* 408 (1986) 165.
- [4] J.M. Ottino, *The Kinematics of Mixing: Stretching, Chaos and Transport*, Cambridge University Press, Cambridge, 1989.
- [5] A. Crisanti, M. Falcioni, G. Paladin, A. Vulpiani, *La Riv. Nuovo Cimento* 14 (1991) 207.
- [6] S. Wiggins, *Chaotic Transport in Dynamical Systems*, Springer, Berlin, 1992.
- [7] H. Aref (Ed.), *Chaos applied to fluid mixing*, (special issue) *Chaos Solitons Fractals* 4(6) (1994).
- [8] R.B. Rybka et al., *Phys. Rev. E* 48 (1993) 757.
- [9] T.H. Solomon, J.P. Gollub, *Phys. Rev. A* 38 (1988) 6280.
- [10] T.H. Solomon, E.R. Weeks, H.L. Swinney, *Physica D* 76 (1994) 70.
- [11] R.T. Pierrehumbert, *Chaos Solitons Fractals* 4 (1994) 1091.
- [12] V.V. Meleshko, G.J.F. van Heijst, *Chaos* 4 (1994) 977.
- [13] V.V. Meleshko et al., *Phys. Fluids A* (1992) 2779.
- [14] J.B. Kadtko, E.A. Novikov, *Chaos* 3 (1993) 543.
- [15] J.C. Sommerer, E. Ott, *Science* 259 (1993) 281.
- [16] J.C. Sommerer, *Physica D* 76 (1994) 85.
- [17] D. Beigie, A. Leonard, S. Wiggins, *Chaos Solitons Fractals* 4 (1994) 749.

- [18] H. Aref, S.W. Jones, S. Mofina, I. Zawadski, *Physica D* 37 (1989) 423.
- [19] V. Rom-Kedar, A. Leonard, S. Wiggins, *J. Fluid. Mech.* 214 (1990) 347.
- [20] K. Shariff, T.H. Pulliam, J.M. Ottino, *Lect. Appl. Math.* 28 (1991) 613.
- [21] C. Jung, E. Ziemniak, *J. Phys. A* 25 (1992) 3929.
- [22] C. Jung, T. Tél, E. Ziemniak, *Chaos* 3 (1993) 555.
- [23] E. Ziemniak, C. Jung, T. Tél, *Physica D* 76 (1994) 123.
- [24] Á. Péntek, T. Tél, Z. Toroczkai, *J. Phys. A* 28 (1995) 2191.
- [25] Á. Péntek, T. Tél, Z. Toroczkai, *Fractals* 3 (1995) 33.
- [26] Á. Péntek, Z. Toroczkai, T. Tél, C. Grebogi, J.A. Yorke, *Phys. Rev. E* 51 (1995) 4076.
- [27] G. Károlyi, A. Péntek, T. Tél, Z. Toroczkai, Chaotic tracer dynamics in open hydrodynamical flows, in: E. Infeld, R. Želazny, A. Gałkowski (Eds.), *Proceedings of International Conference on Nonlinear Dynamics, Chaotic and Complex Systems, Zakopane, Poland, 1995*, Cambridge UP, Cambridge, 1997, pp. 24–38.
- [28] J.A. Kennedy, J.A. Yorke, *Topology Appl.* 80 (1997) 201.
- [29] M.A. Sanjuan et al., *Chaos* 7 (1997) 125.
- [30] M.A. Sanjuan et al., *Phys. Rev. Lett.* 78 (1997) 1892.
- [31] G. Károlyi, T. Tél, *Phys. Rep.* 290 (1997) 125.
- [32] A. Provenzale, *Annu. Rev. Fluid. Mech.* 31 (1999) 55.
- [33] A. Babiano, J.H.E. Cartwright, O. Piro, A. Provenzale, preprint, 1999.
- [34] T. Tél, in: Hao Bai-lin (Ed.), *Directions in Chaos, Vol. 3, 1990*, pp. 149–211; STATPHYS'19, World Scientific, Singapore, 1996, pp. 346–362.
- [35] J.C. Sommerer, H.-C. Ku, H.E. Gilreath, *Phys. Rev. Lett.* 77 (1996) 5055.
- [36] S. Edouard, B. Legras, V. Zeitlin, *J. Geophys. Res.* 101 (1996) 16 771.
- [37] M.G. Balluch, P.H. Haynes, *J. Geophys. Res.* 102 (1997) 23 487.
- [38] A. Mariotti, C.R. Mechoso, B. Legras, Ozone filaments from the southern polar night vortex, *J. Geophys. Res.* (1999) submitted for publication.
- [39] M. Van Dyke, *An Album of Fluid Motion*, The Parabolic Press, Stanford, 1982.
- [40] G. Metcalfe, J.M. Ottino, *Phys. Rev. Lett.* 72 (1994) 2875.
- [41] G. Metcalfe, J.M. Ottino, *Chaos, Solitons Fractals* 6 (1995) 425.
- [42] Z. Toroczkai, G. Károlyi, Á. Péntek, T. Tél, C. Grebogi, *Phys. Rev. Lett.* 80 (1998) 500.
- [43] G. Károlyi, Á. Péntek, Z. Toroczkai, T. Tél, C. Grebogi, *Phys. Rev. E* 59 (1999) 5468.
- [44] L.D. Landau, E.M. Lifschitz, *Fluid Mechanics*, Pergamon Press, Oxford, 1987.
- [45] G.E. Hutchinson, *Am. Nat.* 95 (1961) 137.
- [46] G.F. Gause, A.A. Witt, *Am. Nat.* 69 (1935) 596.
- [47] G. Hardin, *Science* 131 (1960) 1292.
- [48] I. Scheuring, G. Károlyi, Á. Péntek, T. Tél, Z. Toroczkai, A model for resolving the plankton paradox: coexistence in open flows, *Freshwater Biol.* (1999), in press.
- [49] W.H. Thomas, C.H. Gibson, *J. Appl. Phycol.* 2 (1990) 71.
- [50] W.H. Thomas, C.H. Gibson, *Deep Sea Res.* 37 (1990) 1583.
- [51] C.H. Gibson, W.H. Thomas, *J. Geophys. Res.* 100 (1995) 24 841.
- [52] S.A. Spall, K.J. Richards, A numerical model of mesoscale frontal instabilities and plankton dynamics, *Deep-Sea Res.*, in press.
- [53] S. Edouard, B. Legras, B. Lefevre, R. Eymard, *Nature* 384 (1996) 444.
- [54] Z. Neufeld, C. López, P.H. Haynes, *Phys. Rev. Lett.* 82 (1999) 2606.